Effects of forced uncoupling protein 1 expression in 3T3-L1 cells on mitochondrial function and lipid metabolism

Yaguang Si,[*] Santhosh Palani,[†] Arul Jayaraman,[†] and Kyongbum Lee[1,§]

Department of Biology* and Department of Chemical and Biological Engineering,[§] Tufts University, Medford, MA 02155; and Department of Chemical Engineering,[†] Texas A&M University, College Station, TX 77843

Abstract **Obesity-related increase in body fat mass is a risk factor for many diseases, including type 2 diabetes. Controlling adiposity by targeted modulation of adipocyte enzymes could offer an attractive alternative to current dietary approaches. Brown adipose tissue, which is present in rodents but not in adult humans, expresses the mitochondrial uncoupling protein 1 (UCP1) that promotes cellular energy dissipation as heat. Here, we report on the direct metabolic effects of forced UCP1 expression in white adipocytes derived from a murine (3T3-L1) preadipocyte cell line. After stable integration, the *ucp1* gene product was continuously expressed during differentiation and reduced the total lipid accumulation by ~30% without affecting other adipocyte markers, such as cytosolic glycerol-3-phosphate dehydrogenase activity and leptin production. The expression of UCP1 also decreased glycerol output and increased glucose uptake, lactate output, and the sensitivity of cellular ATP content to nutrient removal. However, oxygen consumption and β-oxidation were minimally affected. Together, our results suggest that the reduction in intracellular lipid by constitutive expression of UCP1 reflects a downregulation of fat synthesis rather than an upregulation of fatty acid oxidation.**—Si, Y., S. Palani, A. Jayaraman, and K. Lee. **Effects of forced uncoupling protein 1 expression in 3T3-L1 cells on mitochondrial function and lipid metabolism.** ***J. Lipid Res.*** **2007.** 48: **826–836.**

Supplementary key words adipocyte metabolic profile • glucose starvation • cellular ATP content

Obesity and type 2 diabetes have rapidly become leading health problems in the United States (1). Solid epidemiological data have established a positive correlation between the two diseases, which has also been corroborated by molecular evidence (2). Although the cause of type 2 diabetes is multifactorial, it is generally agreed that a reduction in the sensitivity of muscle, liver, and adipose tissue to insulin contributes to disease onset and progression (3). In vivo studies on obesity have shown that systemic insulin resistance is often preceded by the expansion of body fat mass (4), particularly intra-abdominal adiposity (5). In recent years, a growing number of adipocyte-derived metabolic hormones have been identified, notably resistin (6) and adiponectin (7), whose imbalance in obesity likely plays a role in the development of insulin resistance. Other biochemical events and factors include the overproduction of proinflammatory cytokines such as tumor necrosis factor-α (8) and interleukin-6 (9) and the increase of circulating FFAs (10–12). Increasing evidence links high plasma levels of tumor necrosis factor-α and FFAs to hyperglycemia as well as a hypertrophy of the white adipose tissue (WAT) (13), which results from the progressive accumulation of intracellular lipids [triglyceride (TG)]. In obese individuals, circulating FFAs are derived primarily from the lipolysis of TG stored in white adipocytes (14).

Although it shares many features with the WAT, brown adipose tissue (BAT) is specialized for adaptive thermogenesis and expresses high levels of fatty acid oxidation enzymes and mitochondrial respiratory chain components. In particular, the mitochondrial respiratory uncoupling protein 1 (UCP1) is enriched in BAT, whereas it is minimally present in WAT (15). UCP1 is thought to dissipate the mitochondrial membrane potential (MMP), partially uncouple substrate oxidation and oxidative phosphorylation, and promote the dissipation of cellular biochemical energy as heat. Brown fat is present throughout life in rodents but disappears soon after birth in larger

Manuscript received 26 July 2006 and in revised form 20 November 2006 and in re-revised form 2 January 2007.

Published, JLR Papers in Press, January 3, 2007.
DOI 10.1194/jlr.M600343-JLR200

Abbreviations: BAT, brown adipose tissue; FCCP, carbonyl cyanide 4-(trifluoromethoxy) phenylhydrazone; GPDH, glycerol-3-phosphate dehydrogenase; KRH, Krebs-Ringer buffer/HEPES; MMP, mitochondrial membrane potential; OUR, oxygen uptake rate; TG, triglyceride; TMRM, trimethylrhodamine; UCP1, uncoupling protein 1; WAT, white adipose tissue.

[1] To whom correspondence should be addressed.
e-mail: kyongbum.lee@tufts.edu

mammals, including humans. Recent studies have shown that UCP1 may be ectopically induced to express in WAT and thus could be exploited to increase the capacity to oxidize fatty acids in white adipocytes, thereby regulating body fat mass in humans. Induction of UCP1 expression in white adipocytes has been achieved both in vivo and in vitro. For example, the fat-specific ap2 promoter has been used to construct transgenic mice that constitutively express UCP1 in both BAT and WAT (16). These mice were resistant to genetic obesity and carried WAT cells with an increased mitochondrial content. Zucker diabetic fatty rats injected with an adenoviral vector carrying rat leptin cDNA exhibited mitochondrial biogenesis and increased expression of peroxisome proliferator-activated receptor γ coactivator-1α, UCP1, and UCP2 in the WAT (17). In vitro expression of peroxisome proliferator-activated receptor γ coactivator-1α in white adipocytes not only induced UCP1 expression but also stimulated mitochondrial biogenesis and the expression of mitochondrial enzymes of the respiratory chain (18). Silencing of the corepressor protein RIP140 (19) in cultured white adipocytes reduced the expression of lipogenic enzymes and increased the expression of enzymes involved in energy dissipation, including UCP1.

Together, these findings suggested that UCP1 could be an integral component of cellular energy control and that mechanisms of coordinated regulation may exist for UCP1 and other enzymes of oxidative metabolism in white adipocytes. On the other hand, the specific role of UCP1 remains to be fully elucidated. Here, we report on the direct metabolic effects of forced UCP1 expression in white adipocytes. The metabolic phenotype observed in this study, in particular the reduced accumulation of TG, is consistent with the energy-dissipative function of UCP1 in previous reports. Our data also suggest that the reduction in TG reflects a downregulation of fat synthesis rather than an upregulation of fatty acid oxidation.

METHODS

Materials

3T3-L1 cells were obtained from the American Type Culture Collection (Manassas, VA). Tissue culture reagents, including DMEM, calf serum, FBS, human insulin, and penicillin/streptomycin, were purchased from Invitrogen (Carlsbad, CA). [1-^{14}C]2-Deoxy-D-glucose and [U-^{14}C]palmitate were purchased from Perkin-Elmer (Wellesley, MA). Unless noted otherwise, all other chemicals were purchased from Sigma (St. Louis, MO).

Plasmid construction

Plasmids pRevTet-Off and pRevTRE were purchased from BD Biosciences (Mountain View, CA). Plasmid pCMV-Sport6-UCP1 containing the full-length cDNA for mouse *ucp1* was purchased from Invitrogen. The *ucp1* cDNA was excised from pCMV-Sport6-UCP1 by *Sal*I and *Xba* I digestion and subcloned into the *Sal*I and *Xba* I sites of plasmid pSP72 (Promega, Madison, WI) to generate pSP72-UCP1. The UCP1 cDNA was subsequently excised out of pSP72-UCP1 by *Sal*I and *Cla*I digestion and cloned into the *Sal*I and *Cla*I sites of pRevTRE to generate pRevTRE-UCP1.

Electroporation of 3T3-L1 preadipocytes

The pRevTet-Off and pRevTRE-UCP1 plasmids were sequentially introduced into 3T3-L1 preadipocytes by electroporation. Approximately 10 μg of linearized plasmid (using *Sca*I for pRevTet-Off and *BsaA*I for pRevTRE-UCP1) was used for each electroporation. Passage 2 preadipocytes (2.5×10^6) were trypsinized and first electroporated with pRevTet-Off at 950 μF and 240 V in a 0.4 mm cuvette using a Bio-Rad Gene Pulser II (Hercules, CA). After a 10 min recovery at room temperature, the cells were seeded into four T-75 flasks and incubated at 37°C. After 48 h, 700 μg/ml G418-sulfate was applied as selection pressure, and the cells were incubated for 8 days to select for 3T3-L1 preadipocytes that had pRevTet-Off stably integrated into the genome. All surviving cells were pooled, cultivated in a T-75 flask, and electroporated again with either linearized pRevTRE-UCP1 or pRevTRE-null (control) using the same electroporation and selection conditions described above, except that 200 μg/ml hygromycin was used to select for cells that contained either pRevTRE-UCP1 or pRevTRE-null in addition to pRevTet-Off.

Cell culture and differentiation

The double-stable integrated preadipocytes were plated onto 24-well plates and expanded in preadipocyte growth medium consisting of DMEM (high-glucose; 4.5 g/l) supplemented with calf serum (10%, v/v), penicillin (200 U/ml), and streptomycin (200 μg/ml). During this period, medium was replenished every other day. On day 2 after confluence, the cells were induced to differentiate using an adipogenic cocktail (1 μg/ml insulin, 0.5 mM isobutylmethylxanthine, and 1 μM dexamethasone) added to a basal medium (DMEM with 10% FBS and penicillin/streptomycin). After 48 h, the first induction medium was replaced with a second induction medium consisting of the basal adipocyte medium supplemented with only insulin. After another 48 h, the second induction medium was replaced with the basal adipocyte medium. Medium was replenished every other day through day 9 after induction. On day 10 after induction, glucose and serum were withdrawn for 48 h from a randomly selected subset of pRev control and UCP1-expressing cultures. The remaining cultures were fed the basal adipocyte medium with 1% BSA. After this starvation period, all cultures were refed the basal adipocyte medium. The cultures were maintained in this medium for another 48 h, at which time the cultures were terminated.

Microscopy

At the indicated time points, cellular morphology was recorded using phase-contrast microscopy (Nikon US, Melville, NY). The images were analyzed using the SimplePCI software package (Compix, Inc., Cranberry Township, PA). Intracellular lipid droplets were visualized by staining with Oil Red O as described previously (20).

Real-time RT PCR

Total RNA was isolated using the RNeasy Mini Kit from Qiagen (Valencia, CA). The amount of extracted RNA was quantified with the RiboGreen RNA assay kit from Invitrogen. Reverse transcription was performed on a PTC-100 Programmable Thermal Controller (MJ Research, Waltham, MA) using the High-Capacity cDNA Archive Kit (Applied Biosystems, Foster City, CA) with random primers. The UCP1, UCP2, and glycerol-3-phosphate dehydrogenase (GPDH; EC 1.1.1.8) mRNA and 18S rRNA levels were determined using the TaqMan Gene Expression assay (Applied Biosystems). UCP1 and UCP2 mRNA and 18S rRNA were detected and amplified using predesigned primers and

probe sets (Assay on Demand; Applied Biosystems). For GPDH mRNA, the following customized primers and probe were used: 5′-GGTGGACACAGTGGAGATCTG-3′ forward primer, 5′-AGCCAAGCCCATCACAGAAG-3′ reverse primer, and 5′-CCACTATATTCTTCAAGGCCC-3′ probe. All gene expression data were normalized to the 18S rRNA contents in corresponding samples (21).

Western blot

De novo differentiated adipocytes grown in T25 flasks were trypsinized at day 10 after induction and collected by centrifugation at 800 *g* for 10 min at room temperature. Mitochondria were extracted using the Pierce (Rockford, IL) mitochondrial extraction kit. Adipocytes were lysed and differentially centrifuged to separate the nucleus, cytosol, and mitochondrial fractions according to the manufacturer's protocols. Thirty micrograms of mitochondrial proteins was separated by 12% SDS-PAGE and transferred onto nitrocellulose membranes using standard protocols. A goat anti-UCP1 antibody (1:250 dilution) was used as the primary antibody along with a donkey anti-goat secondary antibody (1:5,000 dilution). Both antibodies were purchased from Santa Cruz Biotechnology (Santa Cruz, CA). The blot was developed using the Supersignal Femto West reagent (Pierce) and captured on a Versadoc imager (Bio-Rad).

GPDH enzyme activity and leptin

GPDH activities were measured in situ based on the method of Sottile and Seuwen (22) by monitoring the rate of change of NADH ultraviolet light absorbance at 340 nm in a microplate reader (VERSAmax; Molecular Devices). Activities were normalized with respect to the total protein content (BCA Protein Assay; Pierce) of the corresponding cell samples. Spent medium samples were analyzed for leptin by ELISA (DuoSet ELISA Development System; R&D Systems, Minneapolis, MN).

MMP measurement and MitoTracker Green staining

The polarization of the mitochondrial membrane in the control and UCP-1-expressing cells was determined using trimethylrhodamine (TMRM; Invitrogen). Cells were incubated with 0.5 μM TMRM for 15 min at 37°C and then rinsed once with prewarmed HBSS. After removing the HBSS, the culture plates were immediately placed in a temperature-controlled fluorescence plate reader (Gemini EX; Molecular Devices, Sunnyvale, CA). TMRM fluorescence was measured at 544/590 nm excitation/emission wavelengths. The membrane potential measurements were performed at various times during the glucose withdrawal-addition experiment, as indicated in Results. The fluorescence reading for each well was normalized by the total DNA content of each well. On day 10 after induction, cells were incubated with 200 nM MitoTracker Green FM (Invitrogen) added to the culture medium. After a 60 min incubation at 37°C, the cells were washed once with 1× PBS. Fluorescence was measured immediately after the wash at 490/516 nm excitation/emission.

Metabolite assays

Metabolite measurements were performed on both cell lysates and spent medium samples. Cells were lysed in situ with an SDS buffer solution. TG levels were measured using a commercially available assay (Sigma) that is based on the release of glycerol from TG by lipoprotein lipase. Cellular ATP was measured using a luminescence assay kit (Promega) that is based on the ATP-dependent activity of luciferase. Spent medium samples were collected during the cell culture at various times, as indicated in Results. Immediately after collection, medium samples were briefly centrifuged to remove any cell debris. Glucose and lactate concentrations were measured using enzymatic assays based on the methods of Trinder (23) and Loomis (24), respectively. Free glycerol (unbound to TG) was measured by substituting water for the LPL in the assay reagent mixture. All metabolite data were normalized by the corresponding sample DNA content, which was measured using either Hoechst or PicoGreen (Invitrogen) dye. The PicoGreen dye method was applied to samples used for ATP measurements, because the Hoechst dye interfered with the luminescence assay.

Oxygen uptake

Rates of oxygen consumption were determined using a commercially available biosensor (BD Biosciences) based on the oxygen-sensitive quenching of ruthenium fluorescence. At the time of measurement (day 10 after induction), differentiated pRev control or UCP1 cells were transferred to 96-well plates with a gas-permeable and hydrophobic matrix embedding the fluorescent compound attached to the bottom. Fluorescence readings were taken in a temperature-controlled plate reader (Gemini EX; Molecular Devices) at 10 min intervals for 720 min at excitation and emission wavelengths of 485 and 630 nm, respectively. Before the cell transfer, each plate was preread to determine the baseline fluorescence. Positive controls were established by treating the pRev control adipocytes with 10 or 100 nM FCCP [carbonyl cyanide 4-(trifluoromethoxy)phenylhydrazone]. Sample readings were "double-normalized" first by dividing by the blank plate and then by medium control well readings, as suggested by Guarino et al. (25). The normalized sample readings were converted into relative oxygen consumption rates according to the manufacturer's instructions and normalized by the corresponding DNA content.

Glucose uptake and fatty acid oxidation

On day 10 after induction, rates of glucose transport and β-oxidation were estimated using radioisotope-labeled tracers. The glucose assay was based on the methods of Yu and Zhu (26) with modifications. Briefly, pRev or UCP1-expressing cells on 24-well plates were incubated in a serum-free medium without glucose for 1.5 h. The cells were washed three times and then incubated in Krebs-Ringer buffer/HEPES (KRH) buffer with or without 1 μg/ml insulin. After 15 min, 0.1 μCi of [1-^{14}C]2-deoxy-D-glucose was added per well. After a labeling period of 15 min at 37°C, cells were washed three times with PBS and lysed with an SDS buffer solution. The cell lysates were added to scintillation vials with 10 ml of scintillation fluid (Ultima Gold; Perkin-Elmer). Radioactivity was measured using a liquid scintillation counter (Tri-Carb 1500; Packard Instruments). For the fatty acid assay, a CO_2 evolution-capture system was assembled as described previously (27) with modifications. Adipocytes on 24-well plates were prelabeled with 0.5 μCi/well [U-^{14}C]palmitic acid in 2% FFA-free BSA-KRH buffer. After 30 min, the cells were washed three times and then incubated in the BSA-KRH buffer. The culture plate was then quickly sealed with a rubber gasket. A 24-well filter plate (Unifilter; Perkin-Elmer) was inverted and placed on top of the sealed culture plate such that each well of the filter plate was centered over a hole (5 mm diameter) in the gasket and aligned with a well of the bottom culture plate. Each top well contained a filter paper presoaked with the CO_2 trap solution (β-phenethylamine). The entire assembly was sealed with foam tape. A weight was placed on top to further reduce the potential for leakage. After 2 h at 37°C, 200 μl of 10 N H_2SO_4 was added to each well. After a 12 h incubation at room temperature, the filters were excised from the top plate and placed in scintillation vials. The

vials were completely filled with scintillation fluid and counted for radioactivity.

Statistics

The number of repeats with different populations of cells was at least three for all experiments. The number of technical replicates per experiment is indicated in the figure legends. Comparisons between two experimental groups were performed using ANOVA. Group means were deemed to be statistically significantly different at $P < 0.05$.

RESULTS

Effects of forced UCP1 expression on adipocyte differentiation

To study the direct effects of the brown adipocyte protein UCP1 on white adipocyte metabolism, we stably integrated the *ucp1* gene into 3T3-L1 preadipocytes, which were then subsequently induced to differentiate using the insulin/dexamethasone/isobutylmethylxanthine adipogenic cocktail. These modified cells expressed significantly more *ucp1* mRNA (**Fig. 1A**) than the control cells that had a blank plasmid (pRevTRE-null) stably integrated by electroporation. The expression of UCP1 protein in the mitochondria was also confirmed by Western blot analysis (Fig. 1B). As expected, UCP1 was not detected in the control cells. The forced expression of UCP1 did not significantly alter the mRNA level (Fig. 1A) or enzyme activity (Fig. 1C) of cytosolic GPDH, an adipocyte differentiation marker whose expression is induced by the activation of adipocyte-enriched transcription factors, such as peroxisome proliferator-activated receptor γ (28). UCP1 expression also had no significant effect on the expression of *ucp2* mRNA (Fig. 1A), which is the dominant uncoupling protein in WAT (29). Analysis of the spent adipocyte culture medium for the adipocyte-specific hormone leptin

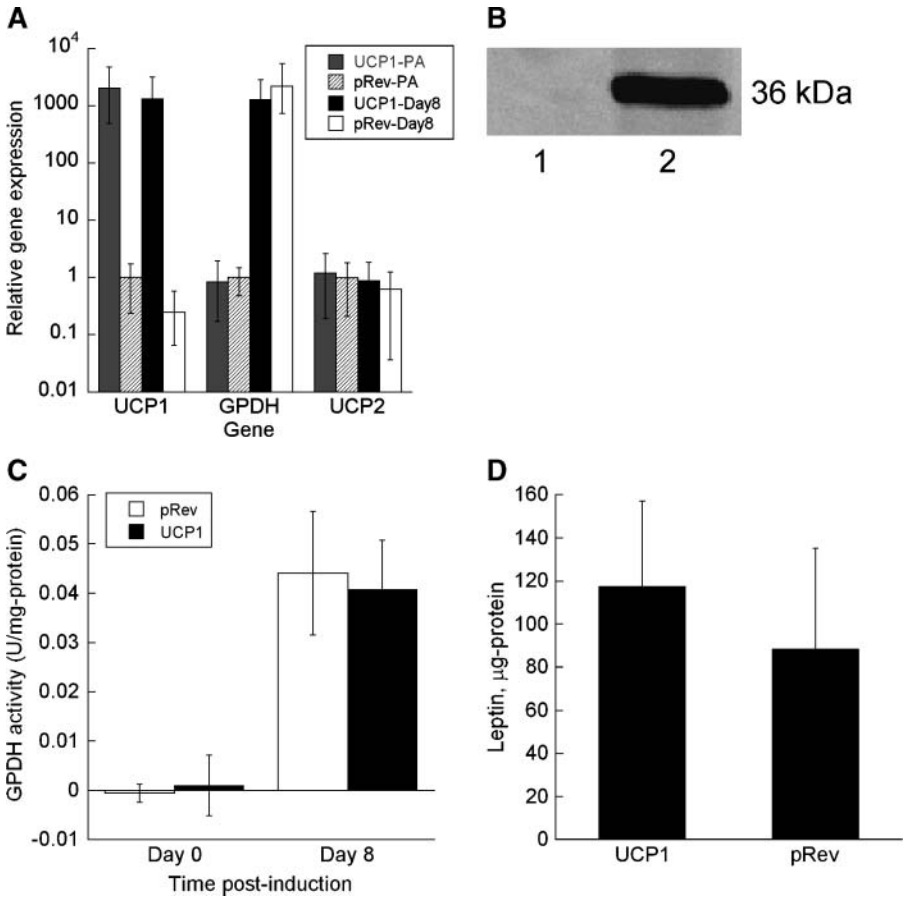

Fig. 1. A: Normalized, relative gene expression levels of uncoupling protein 1 (UCP1; n = 6), glycerol-3-phosphate dehydrogenase (GPDH; n = 3), and UCP2 (n = 7). Values indicate fold changes with respect to the pRev controls as determined from real-time RT-PCR iteration counts for which the corresponding melt curves peaked above a set threshold. Normalization was performed with respect to 18S rRNA. PA, day 2 after confluent preadipocytes; Day8, day 8 after induction. B: Chemiluminescence-based Western blot detection of UCP1. Only the portions corresponding to a molecular mass of ~36 kDa are shown. Lane 1, mitochondrial fraction of null plasmid transfected control cells (pRev); lane 2, mitochondrial fraction of UCP1 transfected cells. C: Enzyme activity of GPDH determined in situ (n = 5). D: Total leptin secreted per well between days 6 and 8 after induction (n = 5). UCP1 and pRev refer to cultures of cells transfected with the target gene and the null plasmid, respectively. Data shown are means ± SD with the indicated number of replicates.

(30) showed no significant differences between UCP1-expressing and control cells (Fig. 1D). The expression level and activity of GPDH increased significantly ($P < 0.05$) with terminal differentiation of either the control or UCP1-expressing preadipocytes. Together, these results suggested that the UCP1 forced expression did not result in an obvious impairment of differentiation.

Reduced adipocyte lipid storage

Morphological assessment by microscopy showed gross differences between the UCP1-expressing cells (**Fig. 2A, B, E, F**) and control cells (Fig. 2C, D, G, H). Consistent with the established phenotype of 3T3-L1 cells (31), the control cells exhibited round shapes and contained visible lipid droplets by day 4 after induction with the adipogenic cocktail. Although the UCP1 cells were also round, Oil Red O-stained images (Fig. 2F, H) showed that by day 8 after induction, a noticeably smaller fraction of the culture contained visible lipid droplets. To quantify the reduction in lipid accumulation, the TG contents of the UCP1 and control cells were measured using an enzymatic assay. On day 10 after induction, cells were subjected to a 2 day treatment with glucose-free medium, after which they were refed the basal adipocyte medium with 4.5 g/l glucose. As shown in **Fig. 3**, the UCP1 cells contained significantly less TG ($P < 0.05$) than the control cells throughout the duration of the experiment. The TG content (expressed as g glycerol/g DNA) of both cultures declined during the glucose-deprivation period, from 1.57 ± 0.24 and 0.91 ± 0.11 at 24 h to 1.30 ± 0.24 and 0.86 ± 0.32 at 48 h for the control and UCP1 cells, respectively. Refeeding the cells with the high-glucose

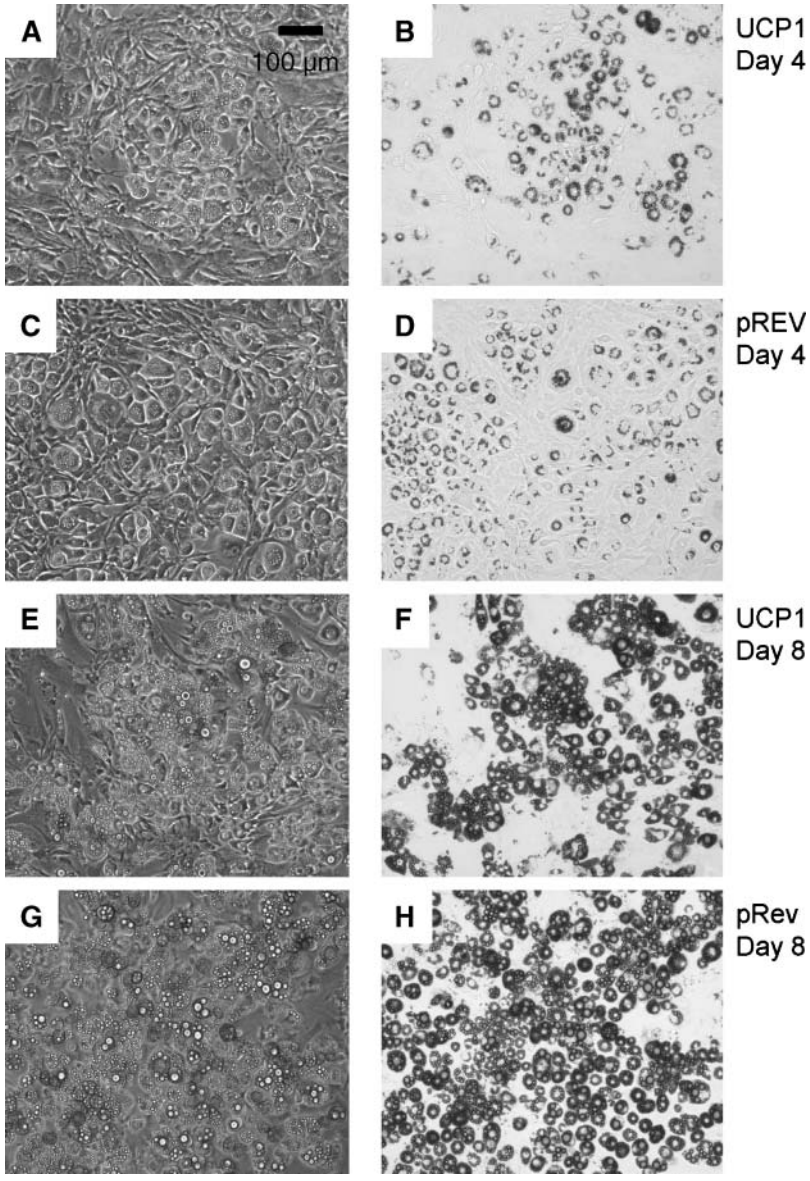

Fig. 2. Phase contrast (A, C, E, G) and Oil Red O-stained (B, D, F, H) images of UCP1 and control (pRev) cells on days 4 and 8 after induction. Times and cell types are as indicated.

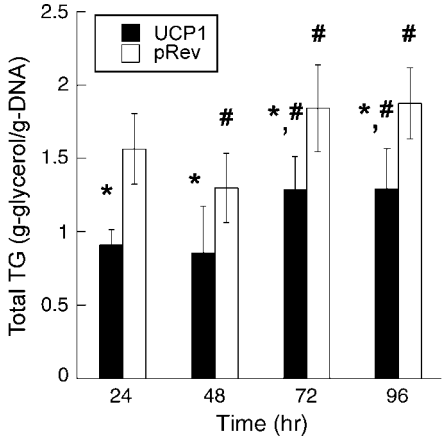

Fig. 3. Effects of forced UCP1 expression on intracellular triglyceride (TG) content (n = 12). The starvation period was from time 0 to 48 h. Data shown are means ± SD. * Statistically significantly different from control (pRev) at $P < 0.05$; # statistically significantly different from the initial value (24 h) of each cell type at $P < 0.05$.

medium increased the TG content of the control and UCP1 cells to 1.84 ± 0.30 and 1.29 ± 0.23, respectively, at 72 h. These amounts were significantly greater ($P < 0.05$) than the corresponding 48 h values and remained approximately stable during the subsequent 24 h.

Reduced oxidative phosphorylation

To explore the biochemical basis for the decrease in TG upon UCP1 expression, we performed a series of metabolic comparisons between the control and UCP1 adipocytes. We first tested for the native activity of the uncoupling protein by assessing the MMP and cellular ATP content. In brown adipocytes, UCP1 facilitates proton conductance across the inner mitochondrial membrane and thereby favors energy dissipation as heat. The MMP and ATP levels were monitored over the course of a 2 day glucose deprivation/2 day refeeding period to also assess the potential contribution of nonmitochondrial pathways, particularly glycolysis, to cellular ATP content. Comparing UCP1 adipocytes with control cells, no significant differences in TMRM fluorescence were observed at any point during the course of the experiment (**Fig. 4A**). The ATP content (expressed as mmol/g DNA) of both the control and UCP1 cells decreased during the starvation period and leveled off after the medium glucose was reintroduced (Fig. 4B). However, the decrease in ATP was significantly greater for the UCP1 cells, reaching 45% of the initial (start of glucose withdrawal) value by 60 h, compared with almost 60% for the control cells. These data indicated that the ability of UCP1-expressing cells to maintain ATP levels similar to the control cells depended more on glucose availability.

When glucose, and hence glycolysis, is no longer available, the most likely source of ATP is the TCA cycle with fatty acid-derived acetyl-CoA as input. The larger reduction in ATP for the UCP1 cells during the glucose withdrawal suggested that oxidative phosphorylation via the TCA cycle was less efficient and/or active compared with the control cells. To compare TCA cycle-driven substrate oxidation in the UCP1 and control adipocytes, we determined their relative rates of oxygen consumption using a fluorescence-based sensor-culture plate. Plots of oxygen uptake rate (OUR) versus time (**Fig. 5A**) showed similar rates for the UCP1-expressing and control cells. As expected, short-term treatment with the chemical uncoupler FCCP increased oxygen consumption in a dose-dependent manner. A comparison of mitochondrial content using a fluorescent stain showed no significant difference between UCP1-expressing and control adipocytes (Fig. 5B).

Metabolic profile

To further investigate the increased dependence on anaerobic pathways for ATP maintenance by the UCP1-

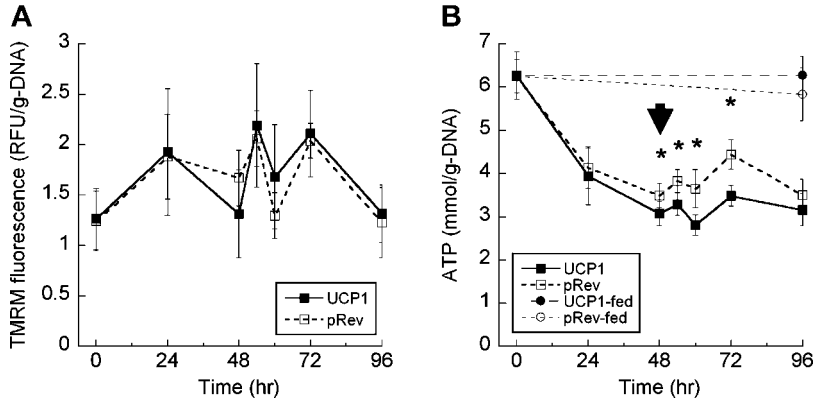

Fig. 4. Effects of forced UCP1 expression on mitochondrial membrane potential (n = 8) (A) and intracellular ATP level (n = 6) (B). The starvation period was from time 0 to 48 h. The arrows indicate the time at which the cells were refed with the basal adipocyte medium containing 4.5 g/l glucose. Data shown are means ± SD with the indicated number of replicates. UCP1-fed and pRev-fed, respectively, refer to UCP1 and pRev control cultures that were not subjected to the glucose starvation. * Statistically significantly different from the pRev control at the same time point at $P < 0.05$. RFU, relative fluorescent unit.

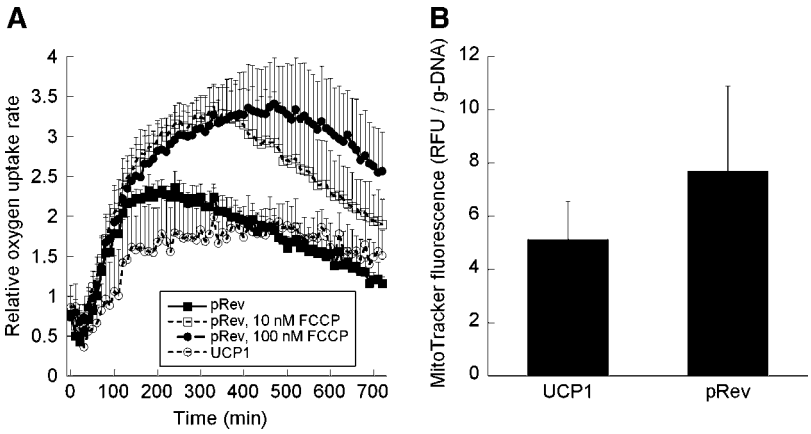

Fig. 5. Effects of forced UCP1 expression on rates of oxygen uptake (n = 6) (A) and mitochondrial content (n = 3) FCCP, carbonyl cyanide 4-(trifluoromethoxy) phenylhydrazone (B). Numbers in (A) refer to final FCCP concentrations in the incubation medium. Data shown are mean ± SD with the indicated number of replicates. Rates were normalized with respect to blank plate, medium control, and DNA content per well as described in Methods. RFU, relative fluorescent unit.

expressing cells, we measured glucose uptake, lactate output, glycerol output, and fatty acid oxidation. Statistically significant differences were observed for glucose, lactate, and glycerol measurements before, during, and after glucose deprivation. Before the starvation period, the UCP1 cells consumed glucose at a significantly higher rate (in g glucose/g DNA/h) of 0.60 ± 0.18 compared with 0.25 ± 0.17 for the control cells (**Fig. 6A**, inset). Upon reexposure to the basal culture medium, the net uptake rates of glucose increased sharply for both the UCP1 and control cells, peaking at 7.17 ± 1.11 and 5.86 ± 1.02, respectively, at 6 h after the refeeding. The glucose uptake rates declined steadily thereafter but remained 3- to ~7-fold higher than the prestarvation levels by day 2 of the refeeding. Radioisotope-labeled tracer experiments with [1-^{14}C]2-deoxy-D-glucose showed that the increase in medium glucose consumption was not attributable to differences in glucose transporter activity. Neither basal nor insulin-stimulated uptake of the nonmetabolized glucose analog was statistically significantly different between the UCP1-expressing and control cells (Fig. 6B). The increase in glucose uptake upon insulin stimulation was ~2-fold, consistent with data reported by others (32). The trends for lactate output were similar to the glucose uptake trends, increasing sharply upon refeeding, with a significantly greater, 1.4-fold increase by the UCP1 cells over the control cells by 72 h (Fig. 6C).

As TG accumulation results from a net difference in synthesis and breakdown, we also examined indicators for FFA release and oxidation. The rates of glycerol release into the medium were measured to determine whether the UCP1 cells have a higher rate of lipolysis than the control cells, as adipocytes normally cannot recycle the free glycerol derived from TG breakdown. The glycerol output rates of the UCP1 cells remained significantly lower than those of the control cells throughout the course of these experiment (Fig. 6D), approximately proportional to their respective TG contents (Fig. 3), indicating that the higher glucose utilization by the UCP1 cells was not correlated with a higher turnover between TG and FFAs. Finally, we compared the relative rates of β-oxidation to determine whether the reduction in TG accumulation could be explained by increased intracellular breakdown of FFAs. Radioisotope-labeled tracer experiments with [U-^{14}C]palmitate showed no significant difference between the relative rates of fatty acid oxidation, suggesting that enhanced lipolysis was unlikely to account for the observed difference in TG accumulation (Fig. 6E).

DISCUSSION

In this work, we have succeeded in forcibly expressing UCP1 in an established in vitro model for adipogenesis. After differentiation by a standard chemical cocktail, the UCP1-expressing cells accumulated significantly less TG than null-plasmid-containing control cells, whereas no significant differences were observed for the following adipocyte differentiation markers: leptin secretion, GPDH gene expression, and GPDH enzyme activity. To explore the metabolic basis for the reduced TG accumulation, we characterized the response of the UCP1 cells to a simple nutritional stress (i.e., starvation). The metabolic profiles determined in this study suggested that attenuation in TG loading may result from an increased demand for carbon flux through glycolysis, as opposed to an upregulation of TG breakdown and fatty acid oxidation. When glucose was withdrawn, stored TG was consumed as fuel in both the UCP1-expressing and control cells, as indicated by the significant reduction in their intracellular TG contents (Fig. 3). During the period without medium glucose, lipogenesis should be minimal, and the products of lipolysis and β-oxidation are likely oxidized through the TCA cycle. Thus, starvation increases the dependence of cellular ATP

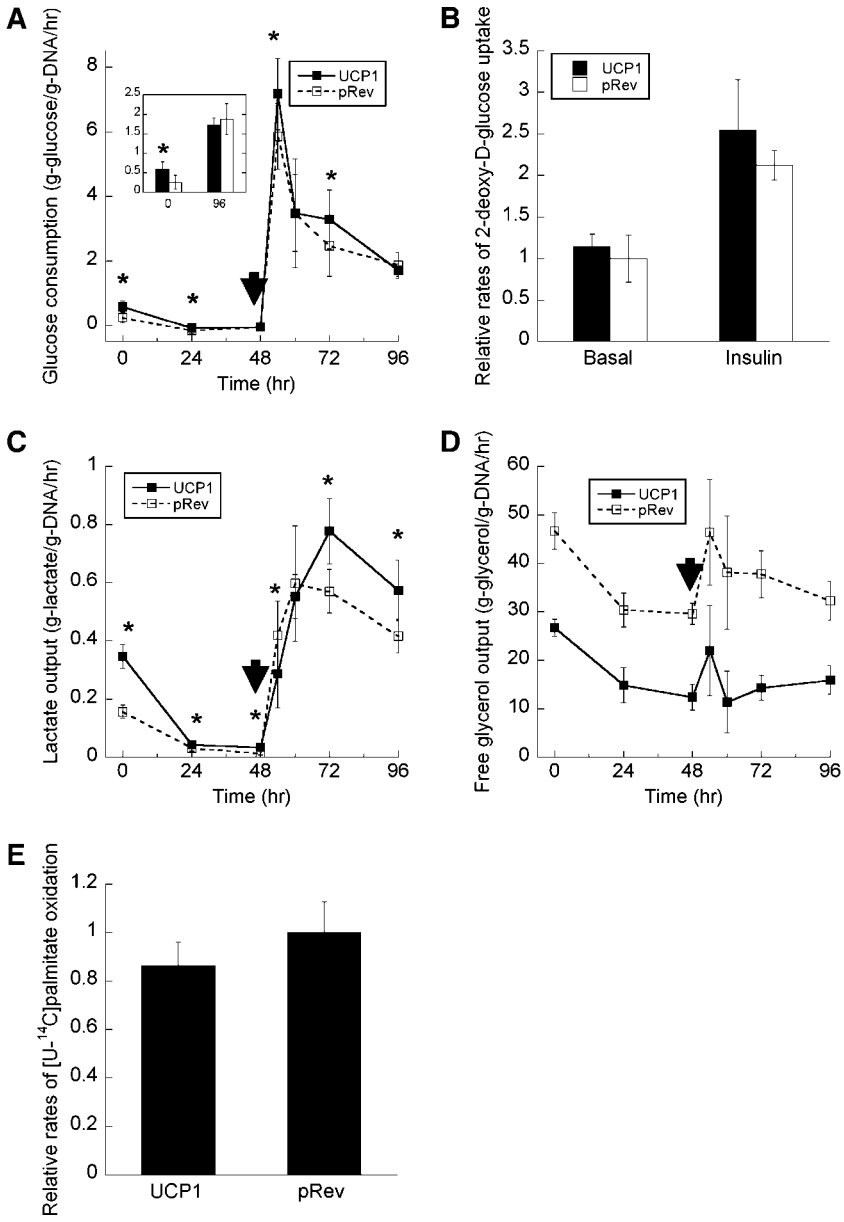

Fig. 6. Effects of forced UCP1 expression on the rates of net glucose consumption (n = 14) (A), [1-^{14}C]2-deoxy-D-glucose uptake (n = 4) (B), lactate output (n = 16) (C), glycerol output (n = 16) (D), and [U-^{14}C]palmitate oxidation (n = 4) (E). The starvation period was from time 0 to 48 h. The arrows indicate the time at which the cells were refed with the basal adipocyte medium containing 4.5 g/l glucose. Data shown are means ± SD with the indicated number of replicates. * Statistically significantly different from the pRev control at the same time point at $P < 0.05$.

maintenance on oxidative phosphorylation, whose decreased efficiency should lead to a greater decrease in ATP content in UCP1-expressing cells, consistent with our findings (Fig. 4B). When provided with medium glucose, the UCP1-expressing cells maintained similar ATP levels as the control cells while consuming more glucose for glycolysis, again suggesting a downregulation of mitochondrial ATP production.

Based on these results, one potential explanation for the reduction in TG synthesis involves an inhibition of the ATP-dependent pyruvate carboxylase, which would decrease the mitochondrial pool of oxaloacetate and citrate and thereby suppress the activity of the malate cycle, which in adipocytes supplies a quantitatively significant fraction of the NADPH needed for de novo fatty acid synthesis (33, 34). Another possibility is that the decreased phosphorylation efficiency drains carbon flux away from storage (lipogenesis) toward the fueling pathways (glycolysis and TCA cycle). These hypotheses warrant further investigation in future studies involving the quantification of metabolic fluxes in intact cells, for example, using isotopic tracers.

The expression of UCP1 in WAT has been the subject of a number of in vivo (16, 35–39) and in vitro (17, 19) studies. Many of these studies have used various upstream

factors for the gene expression and thus cannot be compared directly with this work. The most similar model system involved the expression of the *ucp1* gene from the *ap2* promoter in transgenic mice, which resulted in a targeted increase of UCP1 in WAT (16). In white adipocytes isolated from the *ap2-ucp1* mice, noradrenaline-stimulated lipolysis was impaired (40), and the attenuation in lipid accumulation was mainly attributable to a decrease in FA synthesis (34), which agrees with the findings of this study. On the other hand, the OUR of an incubation of epididymal fat of *ap2-ucp1* transgenic mice showed a significant increase compared with that of controls (41). An increase in oxygen uptake has also been reported for direct, forced expression of UCP1 in HeLa cells (42). In this work, we found that the OUR was not significantly affected by the forced, constitutive expression of UCP1. A likely reason for this apparent discrepancy is that the aforementioned studies used different experimental parameters. Oxygen uptake data on *ap2-ucp1* adipocytes were obtained using fat tissue fragments freshly isolated from 9 month old mice. In addition to the confounding influences of in vivo development and tissue heterogeneity, the fat fragments had been conditioned in plasma containing glucose as well as other nutrients, including FFAs, whereas the cultured adipocytes used in this study relied solely on medium glucose as nutrient fuel. Thus, the *ap2-ucp1* adipocytes could have contained a larger pool of FFAs available for β-oxidation, allowing full compensation for the respiratory uncoupling through an increased supply of acetyl-CoA units. Measurements of oxygen uptake by UCP1-expressing HeLa cells were performed 6 h after the induction of gene expression, whereas this study was carried out with a stable cell line that constitutively expressed UCP1 after several weeks of selection and culture. Sufficient time had passed for the engineered adipocytes to undergo long-term metabolic adaptations, for example, by adjusting the activities of glycolytic enzymes. A number of different cell types have been shown to respond to persistent respiratory uncoupling by first upregulating glucose consumption and anaerobic ATP synthesis and then downregulating oxidative phosphorylation. For example, treatment with rotenone (43), cyanide (44), DNP (33, 34, 45), and hypoxia (46) resulted in an upregulation of glucose uptake. In tumor cells, a prolonged treatment with FCCP also brought about an inhibition of mitochondrial respiration (47).

Finally, the TMRM measurements of this study did not indicate significant differences in the MMP of the UCP1-expressing and control cells, although a putative direct function of UCP1 is to facilitate the influx of protons across the inner mitochondrial membrane. Assuming that UCP1 functions similarly in 3T3-L1 adipocytes as it does in brown adipocytes, it should decrease the MMP, at least in the short term. A decrease in MMP should decrease ATP synthesis and/or cause the reversal of the ATP synthase (48–50), both of which would impair the mitochondrial ATP generation. A reversal of the synthase activity would lead to ATP hydrolysis and the transport of protons out of the inner mitochondria. This proton efflux, which contributes to the membrane gradient at the expense of ATP, could explain the apparent lack of difference between the MMP of UCP1-expressing and control cells (Fig. 4A). Brown adipocytes can compensate for the decrease in MMP by upregulating β-oxidation and the TCA cycle to generate extra NADH and $FADH_2$ for electron transport and oxidative phosphorylation. This was likely not the case here, as the OUR data (Fig. 5A) did not support an increase in aerobic metabolism of the UCP1-expressing 3T3-L1 adipocytes. One explanation is that mature adipocytes have only a limited capacity to oxidize their fat stores (51). Instead, the UCP1-expressing white adipocytes may instead upregulate glycolysis to supplement ATP production. This type of compensation may be especially effective when an abundance of medium glucose allows a trade-off between the ATP yield (higher for oxidative phosphorylation) in favor of the production rate (higher if both aerobic and anaerobic pathways are used) (52). Several earlier studies of the impairment of mitochondrial metabolism have also noted that glycolytic ATP generation is critical to cell survival (53–55).

Long term, the lower ATP yield incurred through an increased utilization of glycolysis may eventually prevent the UCP1-expressing white adipocytes from completely compensating for the reduced mitochondrial supply of ATP. This could force the UCP1 cells to adapt by downregulating the ATP-using pathways. Buttgereit and Brand (56) have suggested that there exists a hierarchy of responses by the different energy-consuming reactions to changes in energy supply, in which the pathways of macromolecular biosynthesis are the most sensitive to limited ATP supply. Our own observations suggested that the UCP1-expressing preadipocytes grew more slowly than the control cells (unpublished data).

In summary, the findings in this study suggest that the major direct effect of UCP1 on white adipocyte metabolism is to reduce TG accumulation through a downregulation of several energy- and carbon flux-requiring processes. We hypothesize that the chronic overexpression of UCP1 brought about an increase in the relative contribution of glycolysis to total ATP production. The findings in this study provide further evidence that the specific induction of a single adipocyte protein, UCP1, could provide a potential approach for controlling adipose tissue fat accumulation. Prospectively, this approach may offer clinically useful features, as simultaneous reduction in body adiposity and blood glucose are desired outcomes of therapies for obesity-related diabetes.

The authors gratefully acknowledge Dr. Joseph Platko for his assistance with electroporation, Andrew Wood for his help with the Oil Red O stains, and Diah Bramono for her technical support of the real-time RT-PCR equipment. The authors thank Dr. Gregory Stephanopoulos and Keith Tyo for the use of facilities in performing the radioactive tracer experiments. This work was supported by grants from the National Institutes of Health (1 R21 DK-67228-01) and the Tufts University Faculty Research Fund to K.L. and from the Texas Engineering Experiment Station to A.J.

REFERENCES

1. Wickelgren, I. 1998. Obesity: how big a problem? *Science.* **280:** 1364–1367.
2. Scheen, A. J. 2000. From obesity to diabetes: why, when and who? *Acta Clin. Belg.* **55:** 9–15.
3. Saltiel, A. R. 2001. New perspectives into the molecular pathogenesis and treatment of type 2 diabetes. *Cell.* **104:** 517–529.
4. Colditz, G. A., W. C. Willett, M. J. Stampfer, J. E. Manson, C. H. Hennekens, R. A. Arky, and F. E. Speizer. 1990. Weight as a risk factor for clinical diabetes in women. *Am. J. Epidemiol.* **132:** 501–513.
5. Kissebah, A. H., and G. R. Krakower. 1994. Regional adiposity and morbidity. *Physiol. Rev.* **74:** 761–811.
6. Steppan, C. M., S. T. Bailey, S. Bhat, E. J. Brown, R. R. Banerjee, C. M. Wright, H. R. Patel, R. S. Ahima, and M. A. Lazar. 2001. The hormone resistin links obesity to diabetes. *Nature.* **409:** 307–312.
7. Yamauchi, T., J. Kamon, H. Waki, Y. Terauchi, N. Kubota, K. Hara, Y. Mori, T. Ide, K. Murakami, N. Tsuboyama-Kasaoka, et al. 2001. The fat-derived hormone adiponectin reverses insulin resistance associated with both lipoatrophy and obesity. *Nat. Med.* **7:** 941–946.
8. Hotamisligil, G. S., N. S. Shargill, and B. M. Spiegelman. 1993. Adipose expression of tumor necrosis factor-alpha: direct role in obesity-linked insulin resistance. *Science.* **259:** 87–91.
9. Pickup, J. C., M. B. Mattock, G. D. Chusney, and D. Burt. 1997. NIDDM as a disease of the innate immune system: association of acute-phase reactants and interleukin-6 with metabolic syndrome X. *Diabetologia.* **40:** 1286–1292.
10. Boden, G. 1997. Role of fatty acids in the pathogenesis of insulin resistance and NIDDM. *Diabetes.* **46:** 3–10.
11. Charles, M. A., E. Eschwege, N. Thibult, J. R. Claude, J. M. Warnet, G. E. Rosselin, J. Girard, and B. Balkau. 1997. The role of non-esterified fatty acids in the deterioration of glucose tolerance in Caucasian subjects: results of the Paris Prospective Study. *Diabetologia.* **40:** 1101–1106.
12. Paolisso, G., P. A. Tataranni, J. E. Foley, C. Bogardus, B. V. Howard, and E. Ravussin. 1995. A high concentration of fasting plasma non-esterified fatty acids is a risk factor for the development of NIDDM. *Diabetologia.* **38:** 1213–1217.
13. Yin, W., D. Liao, Z. Wang, S. Xi, K. Tsutsumi, T. Koike, J. Fan, G. Yi, Q. Zhang, Z. Yuan, et al. 2004. NO-1886 inhibits size of adipocytes, suppresses plasma levels of tumor necrosis factor-[alpha] and free fatty acids, improves glucose metabolism in high-fat/high-sucrose-fed miniature pigs. *Pharmacol. Res.* **49:** 199–206.
14. Bergman, R. N., and S. D. Mittelman. 1998. Central role of the adipocyte in insulin resistance. *J. Basic Clin. Physiol. Pharmacol.* **9:** 205–221.
15. Nicholls, D. G., and R. M. Locke. 1984. Thermogenic mechanisms in brown fat. *Physiol. Rev.* **64:** 1–64.
16. Kopecky, J., G. Clarke, S. Enerback, B. Spiegelman, and L. P. Kozak. 1995. Expression of the mitochondrial uncoupling protein gene from the aP2 gene promoter prevents genetic obesity. *J. Clin. Invest.* **96:** 2914–2923.
17. Orci, L., W. S. Cook, M. Ravazzola, M. Y. Wang, B. H. Park, R. Montesano, and R. H. Unger. 2004. Rapid transformation of white adipocytes into fat-oxidizing machines. *Proc. Natl. Acad. Sci. USA.* **101:** 2058–2063.
18. Tiraby, C., G. Tavernier, C. Lefort, D. Larrouy, F. Bouillaud, D. Ricquier, and D. Langin. 2003. Acquirement of brown fat cell features by human white adipocytes. *J. Biol. Chem.* **278:** 33370–33376.
19. Christian, M., E. Kiskinis, D. Debevec, G. Leonardsson, R. White, and M. G. Parker. 2005. RIP140-targeted repression of gene expression in adipocytes. *Mol. Cell. Biol.* **25:** 9383–9391.
20. Hauner, H., T. Skurk, and M. Wabitsch. 2001. Cultures of human adipose precursor cells. *In* Adipose Tissue Protocols. G. Ailhaud, editor. Humana Press, Totowa, NJ. xiii.
21. Schmittgen, T. D., and B. A. Zakrajsek. 2000. Effect of experimental treatment on housekeeping gene expression: validation by real-time, quantitative RT-PCR. *J. Biochem. Biophys. Methods.* **46:** 69–81.
22. Sottile, V., and K. Seuwen. 2001. A high-capacity screen for adipogenic differentiation. *Anal. Biochem.* **293:** 124–128.
23. Trinder, P. 1969. Determination of blood glucose using an oxidase-peroxidase system with a non-carcinogenic chromogen. *J. Clin. Pathol.* **22:** 158–161.
24. Loomis, M. E. 1961. An enzymatic fluorometric method for the determination of lactic acid in serum. *J. Lab. Clin. Med.* **57:** 966–969.
25. Guarino, R. D., L. E. Dike, T. A. Haq, J. A. Rowley, J. B. Pitner, and M. R. Timmins. 2004. Method for determining oxygen consumption rates of static cultures from microplate measurements of pericellular dissolved oxygen concentration. *Biotechnol. Bioeng.* **86:** 775–787.
26. Yu, Y. H., and H. Zhu. 2004. Chronological changes in metabolism and functions of cultured adipocytes: a hypothesis for cell aging in mature adipocytes. *Am. J. Physiol. Endocrinol. Metab.* **286:** E402–E410.
27. Collins, C. L., B. P. Bode, W. W. Souba, and S. F. Abcouwer. 1998. Multiwell $^{14}CO_2$-capture assay for evaluation of substrate oxidation rates of cells in culture. *Biotechniques.* **24:** 803–808.
28. Patsouris, D., S. Mandard, P. J. Voshol, P. Escher, N. S. Tan, L. M. Havekes, W. Koenig, W. Marz, S. Tafuri, W. Wahli, et al. 2004. PPAR{alpha} governs glycerol metabolism. *J. Clin. Invest.* **114:** 94–103.
29. Ricquier, D., and F. Bouillaud. 2000. The uncoupling protein homologues: UCP1, UCP2, UCP3, StUCP and AtUCP. *Biochem. J.* **345:** 161–179.
30. Rentsch, J., and M. Chiesi. 1996. Regulation of ob gene mRNA levels in cultured adipocytes. *FEBS Lett.* **379:** 55–59.
31. Green, H., and O. Kehinde. 1975. An established preadipose cell line and its differentiation in culture. II. Factors affecting the adipose conversion. *Cell.* **5:** 19–27.
32. Lin, Y., A. H. Berg, P. Iyengar, T. K. Lam, A. Giacca, T. P. Combs, M. W. Rajala, X. Du, B. Rollman, W. Li, et al. 2005. The hyperglycemia-induced inflammatory response in adipocytes: the role of reactive oxygen species. *J. Biol. Chem.* **280:** 4617–4626.
33. Rognstad, R., and J. Katz. 1969. The effect of 2,4-dinitrophenol on adipose-tissue metabolism. *Biochem. J.* **111:** 431–444.
34. Rossmeisl, M., I. Syrovy, F. Baumruk, P. Flachs, P. Janovska, and J. Kopecky. 2000. Decreased fatty acid synthesis due to mitochondrial uncoupling in adipose tissue. *FASEB J.* **14:** 1793–1800.
35. Cabrero, A., G. Llaverias, N. Roglans, M. Alegret, R. Sanchez, T. Adzet, J. C. Laguna, and M. Vazquez. 1999. Uncoupling protein-3 mRNA levels are increased in white adipose tissue and skeletal muscle of bezafibrate-treated rats. *Biochem. Biophys. Res. Commun.* **260:** 547–556.
36. Emilsson, V., J. O'Dowd, S. Wang, Y. L. Liu, M. Sennitt, R. Heyman, and M. A. Cawthorne. 2000. The effects of rexinoids and rosiglitazone on body weight and uncoupling protein isoform expression in the Zucker fa/fa rat. *Metabolism.* **49:** 1610–1615.
37. Fukui, Y., S. Masui, S. Osada, K. Umesono, and K. Motojima. 2000. A new thiazolidinedione, NC-2100, which is a weak PPAR-gamma activator, exhibits potent antidiabetic effects and induces uncoupling protein 1 in white adipose tissue of KKAy obese mice. *Diabetes.* **49:** 759–767.
38. Matsuda, J., K. Hosoda, H. Itoh, C. Son, K. Doi, I. Hanaoka, G. Inoue, H. Nishimura, Y. Yoshimasa, Y. Yamori, et al. 1998. Increased adipose expression of the uncoupling protein-3 gene by thiazolidinediones in Wistar fatty rats and in cultured adipocytes. *Diabetes.* **47:** 1809–1814.
39. Wilson-Fritch, L., S. Nicoloro, M. Chouinard, M. A. Lazar, P. C. Chui, J. Leszyk, J. Straubhaar, M. P. Czech, and S. Corvera. 2004. Mitochondrial remodeling in adipose tissue associated with obesity and treatment with rosiglitazone. *J. Clin. Invest.* **114:** 1281–1289.
40. Flachs, P., J. Novotny, F. Baumruk, K. Bardova, L. Bourova, I. Miksik, J. Sponarova, P. Svoboda, and J. Kopecky. 2002. Impaired noradrenaline-induced lipolysis in white fat of aP2-Ucp1 transgenic mice is associated with changes in G-protein levels. *Biochem. J.* **364:** 369–376.
41. Kopecky, J., M. Rossmeisl, Z. Hodny, I. Syrovy, M. Horakova, and P. Kolarova. 1996. Reduction of dietary obesity in aP2-Ucp transgenic mice: mechanism and adipose tissue morphology. *Am. J. Physiol.* **270:** E776–E786.
42. Li, B., J. O. Holloszy, and C. F. Semenkovich. 1999. Respiratory uncoupling induces delta-aminolevulinate synthase expression through a nuclear respiratory factor-1-dependent mechanism in HeLa cells. *J. Biol. Chem.* **274:** 17534–17540.
43. Bashan, N., E. Burdett, A. Guma, R. Sargeant, L. Tumiati, Z. Liu, and A. Klip. 1993. Mechanisms of adaptation of glucose transporters to changes in the oxidative chain of muscle and fat cells. *Am. J. Physiol.* **264:** C430–C440.
44. Mercado, C. L., J. N. Loeb, and F. Ismail-Beigi. 1989. Enhanced glucose transport in response to inhibition of respiration in Clone 9 cells. *Am. J. Physiol.* **257:** C19–C28.
45. Kang, J., E. Heart, and C. K. Sung. 2001. Effects of cellular ATP depletion on glucose transport and insulin signaling in 3T3-L1 adipocytes. *Am. J. Physiol. Endocrinol. Metab.* **280:** E428–E435.

46. Zhang, J. Z., A. Behrooz, and F. Ismail-Beigi. 1999. Regulation of glucose transport by hypoxia. *Am. J. Kidney Dis.* **34:** 189–202.
47. Gabai, V. L. 1993. Inhibition of uncoupled respiration in tumor cells. A possible role of mitochondrial Ca^{2+} efflux. *FEBS Lett.* **329:** 67–71.
48. Jennings, R. B., K. A. Reimer, and C. Steenbergen. 1991. Effect of inhibition of the mitochondrial ATPase on net myocardial ATP in total ischemia. *J. Mol. Cell. Cardiol.* **23:** 1383–1395.
49. St-Pierre, J., M. D. Brand, and R. G. Boutilier. 2000. Mitochondria as ATP consumers: cellular treason in anoxia. *Proc. Natl. Acad. Sci. USA.* **97:** 8670–8674.
50. Vinogradov, A. D. 2000. Steady-state and pre-steady-state kinetics of the mitochondrial F(1)F(o) ATPase: is ATP synthase a reversible molecular machine? *J. Exp. Biol.* **203:** 41–49.
51. Wang, T., Y. Zang, W. Ling, B. E. Corkey, and W. Guo. 2003. Metabolic partitioning of endogenous fatty acid in adipocytes. *Obes. Res.* **11:** 880–887.
52. Pfeiffer, T., S. Schuster, and S. Bonhoeffer. 2001. Cooperation and competition in the evolution of ATP-producing pathways. *Science.* **292:** 504–507.
53. Gajewski, C. D., L. Yang, E. A. Schon, and G. Manfredi. 2003. New insights into the bioenergetics of mitochondrial disorders using intracellular ATP reporters. *Mol. Biol. Cell.* **14:** 3628–3635.
54. Nieminen, A. L., A. K. Saylor, B. Herman, and J. J. Lemasters. 1994. ATP depletion rather than mitochondrial depolarization mediates hepatocyte killing after metabolic inhibition. *Am. J. Physiol.* **267:** C67–C74.
55. Snyder, J. W., J. G. Pastorino, A. P. Thomas, J. B. Hoek, and J. L. Farber. 1993. ATP synthase activity is required for fructose to protect cultured hepatocytes from the toxicity of cyanide. *Am. J. Physiol.* **264:** C709–C714.
56. Buttgereit, F., and M. D. Brand. 1995. A hierarchy of ATP-consuming processes in mammalian cells. *Biochem. J.* **312:** 163–167.